Energy Engineering

Tech Science Press

DOI: 10.32604/ee.2022.019331

ARTICLE

Numerical Study on Heat Transfer Characteristic of the Plate-Fin Microchannel Heat Sink for Water-Based Thermal Management of CPU Chip

Jie-Chao Chen, Rui-Hao Luo, Wu-Zhi Yuan, Nan-Long Hong* and Wen-Hao Wang

Guangdong Provincial Key Laboratory of Distributed Energy Systems, Guangdong Provincial Engineering Research Center of Distributed Energy Systems, Dongguan University of Technology, Dongguan, 523808, China

*Corresponding Author: Nan-Long Hong. Email: hongnl@dgut.edu.cn

Received: 17 September 2021 Accepted: 16 November 2021

ABSTRACT

For effective water-based thermal management of high heat generating CPU chip, a series of numerical simulation has been conducted to study the effects of heat flux, fin height and flow rate on convective thermal performance of the plate-fin microchannel heat sinks. The characteristics of heat transfer and flow resistance have been quantificationally discussed and *JF* factor is employed to evaluate the comprehensive efficiency of convective heat transfer of microchannel heat sink. Results show that the increase in fin height and flow rate of cooling water is helpful to decrease the maximum temperature of CPU chip. Large flow rate and heat flux and short fin height are benefit to improve Nusselt number *Nu*, but they lead to large resistance coefficient *fRe* simultaneously. Analysis of *JF* factor shows that the microchannel with short fins shows better convective thermal performance when the thermal power of the CPU chip is small. The fins should be heightened when the CPU is operating at higher thermal power. The employment of *JF* factor in the present work shows its pertinence and convenience in the application of design of microchannel heat sink.

KEYWORDS

JF factor; convective thermal performance; numerical simulation; thermal management of CPU

1 Introduction

In recent years, the progress of computer technology constantly has pushed urgent requirements for the update of high performance chips, which resulting in a dramatic increase in the number of transistors inside a CPU [1,2]. In the design of the computing system, the cooling ability of chip becomes more and more important. At present, the mainstream commercial CPU chip power is up to 125 W. Traditional thermal management methods for CPU cannot be appropriate for such high heat flux. The limit of fan-fin cooling techniques is 50 W/cm^2 due to fin efficiency and heat spreading bottlenecks. There are disproportionately large increases in pressure drop and acoustic noise with modest gains in heat transfer. Therefore, it will not be a valid solution [3]. One of the solutions proposed is to further enhance the heat transfer by utilizing microchannel heat sink in a liquid-based system since its high heat dissipation performance [4,5]. Liquid based cooling heat sink affords reasonable heat transfer coefficients in dealing with the heat dissipation problem of chips. The heat is extracted from the board by one heat sink and released to the air by another remote heat sink. It is accepted that the form factor constraints of liquid based cooling are not as severe [6,7].

Over the past 20 years, previous studies have shown that the water-based microchannel heat sink has high heat transfer surface areas per unit volume. However, its drawback is undesirable temperature gradients from inlet to outlet caused by the mono-directional fluid flow. Therefore, the layout of microchannel of the heat sink is very important for the thermal management design [8]. Numerous researchers have performed investigations on the optimal performance of water-based microchannel heat sink. By reducing the hydraulic diameter and changing the geometrical factors, including cross-sectional shape, pattern, manifold and input/output ports, optimization of average temperature, pressure drop, heat transfer coefficient, Nusselt number, as well as flow and temperature uniformity have been achieved [9]. Toh et al. [10,11] respectively conducted the numerical and experimental studies on the fluid flow and heat transfer in four kinds of straight microchannel. Results show that the temperature of the water increases, leading to a decrease in the viscosity and hence smaller frictional losses, particularly at lower Reynolds numbers. Ying et al. [12] numerically investigated the heat transfer performance of microchannel heat sinks with a length of 40 mm and different cross-sectional dimensions. The result shows rectangle structures have smaller pressure drop but higher heat transfer efficiency compared with the triangle and trapezoid shapes. Xie et al. [13] numerically investigated straight and rectangular microchannel heat sinks with different length bifurcation and dimension. Results show that proper design of the multiple length bifurcation could be employed to improve the overall thermal performance of microchannel heat sinks. Liang et al. [14] proposed to enhance heat transfer by equipping pin-fins in the channel walls of microchannel. However, the fluidity of the fluid flow is reduced. Therefore, in the design of microchannel heat sink, it is required to consider thermo-hydraulic performance, and fabrication capability [9], which means a balance between heat transfer enhancement and pressure drop penalty.

There are some parameters such as Performance Evaluation Criteria (PEC) which could be useful to specify crucial parameters [15,16]. Performance evaluation criteria (PEC) is calculated by using extracted data to achieve better decision from the perspective of cross-section and pattern of the microchannel heat sink. Liu et al. [17] proposed a novel microchannel sink with perforated baffles and perforated walls (MSPBPW) to ameliorate the bottom surface temperature of the heat sink. It is found that the heat transfer ability of MSPBPW with pressure drop penalty can be significantly improved, and the thermal performance evaluation criterion value is always greater than unity. Mazloumi et al. [18] evaluated the hydrothermal performance between plate fins and plate-pin fins subject to nanofluid-cooled corrugated miniature heat sinks. The maximum hydrothermal performance factor of 1.84 is detected for 0.3% nanofluid flow in the corrugated miniature heat sink with sinusoidal plate-pin fins. Additionally, it is noted that the *JF* factor is an important and common parameter in the application of the evaluation criteria for the overall thermal performance of different heat exchangers [19–21]. The *JF* factor can not only provide quantitative comparison of the simultaneous effect of heat transfer and friction, but also help to determine the key influence parameters of the research object.

The objective of the present study is to utilize the evaluation criteria *JF* factor to analyze the hydrothermal performance of the microchannel heat sink with straight fins. A series of numerical investigations on the velocity field and distributions of temperature and pressure for the water-based microchannel heat sink with various fin height, flow rate and CPU power have been carefully conducted. The present work aims to provide data reference for the design and optimization on configuration of microchannel heat sink.

2 Numerical Simulation

2.1 Physical Model

As shown in Fig. 1, the water-based microchannel heat sink with an array of straight fins was constructed [22]. Accordingly, the size difference between the CPU chip (I) and microchannel heat sink (III) is large. It is necessary to set a thermal conductive plate (II) between CPU chip and heat sink for the purpose to reduce the thermal resistance. The water inlet and water outlet are respectively set in the lower left corner and the upper right corner of the heat sink. The inner diameters of the inlet and outlet vents are both 5 mm. The width of each micro channel is 0.9 mm. The convective water extracts the heat from the board of the microchannels and released to the air by another remote heat sink, which results in the cooling effect on the CPU chip. The working fluid is pure water. Its detail thermodynamic properties are as follows: $\lambda = 0.6$ W/(m·K), $\mu = 0.001003$ kg/(m·s), $\rho = 998.2$ kg/m^3, $c_p = 4182$ J/(kg·K), where λ, μ, ρ and c_p refer to thermal conductivity, viscosity, density and specific heat, respectively. The microchannel is made of copper, with $c_p = 385$ J/(kg·K), $\rho = 8960$ kg/m^3 and $\lambda = 400$ W/(m·K). At the inlet vent, the temperature of cooling water flow is 293.15 K. The specific parameters of the straight-fin microchannel heat sink are shown in Table 1.

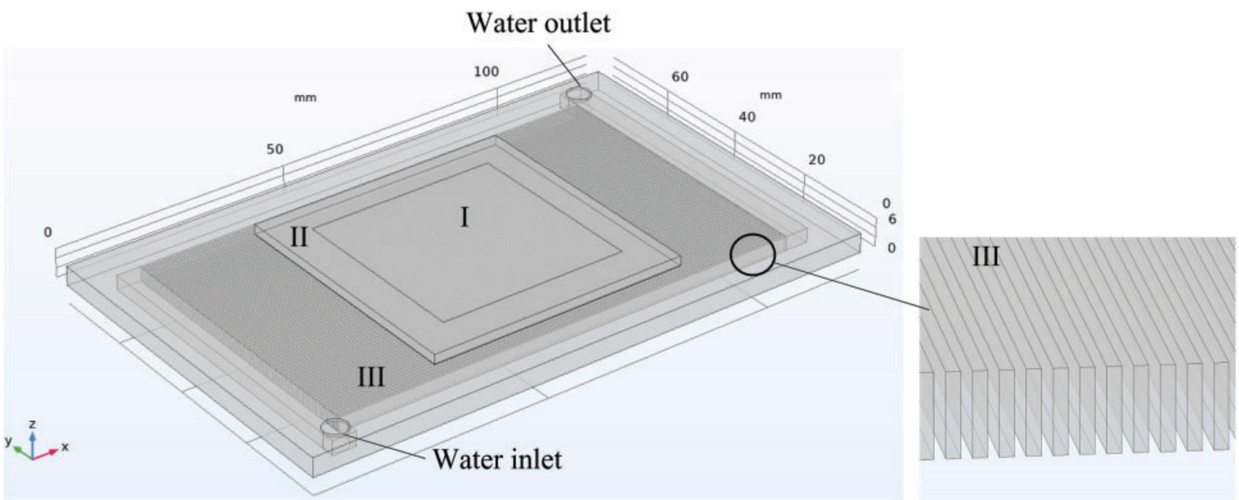

Figure 1: Geometric model of straight-fin microchannel heat sink. (I: bottom face of CPU chip, II: thermal conductive plate, III: microchannel heat sink)

Table 1: Geometry sizes of microchannel heat sinks

Geometry size	Length × Width × Height/mm^3
Microchannel heat sink	122 × 77 × 4
Flow region	100 × 60 × 4
Thermal conductive plate	55 × 55 × 2
CPU chip	40 × 40 × 2

2.2 Governing Equations

In order to simplification, several assumptions were employed. (1) The Reynolds number in the channel bellows 1600 and the fluid flow is laminar and steady flow; (2) Fluid is incompressible, Newtonian, and viscous; (3) There is no velocity-slip at the solid-liquid walls; (4) The density in the momentum equation is assumed to be constant, except that the density in the diffusion term varies with temperature [18–21].

Therefore, the steady-state governing equations for mass, momentum, and energy conservations adopted in the present work are given as follows [23]:

$$\nabla \cdot (\rho \boldsymbol{u}) = 0, \tag{1}$$

$$(\boldsymbol{u} \cdot \nabla)\, \boldsymbol{u} = -\frac{\nabla p}{\rho} + \frac{\mu}{\rho} \nabla^2 \boldsymbol{u}, \tag{2}$$

$$\rho c_{\mathrm{p}} \boldsymbol{u} \cdot \nabla T = \lambda \nabla^2 T, \tag{3}$$

where $\boldsymbol{u}$ denotes the velocities in the three-dimensional coordination, μ, p and T are respectively the dynamic viscosity, pressure and temperature.

Additionally, the Reynolds number Re, the Nusselt number Nu, j factor and the resistance coefficient f are defined as [24]:

$$Re = \frac{\rho u_{\mathrm{ch}} D_{\mathrm{h}}}{\mu}, \tag{4}$$

$$Nu = \frac{h D_{\mathrm{h}}}{\lambda}, \tag{5}$$

$$j = \frac{h Pr^{2/3}}{\rho c_{\mathrm{p}} u_{\mathrm{in}}}, \tag{6}$$

$$f = \frac{p_{\mathrm{out}} - p_{\mathrm{in}}}{\frac{1}{2} \rho u_{in}^2}, \tag{7}$$

in which, u_{ch}, u_{in}, D_{h}, h, Pr, p_{in} and p_{out} respectively refer to velocity in the micro channel, velocity at the inlet, equivalent diameter of the micro channels, convective heat transfer coefficient, the Prandtl number, pressure at the inlet and outlet.

Most of the boundary conditions of the present work are unified setting for the microchannel heat sink with different fin heights. The water flow is fully developed at the inlet vent. Constant heat fluxes are adopted at the top of CPU chip, all of other walls were treated as adiabatic [25].

2.3 Grid Independency

The software utilized to perform the present numerical simulation is COMSOL Multiphysics. The grid verification is performed by adopting the module with fin height of 2 mm, heat flux of 50 W/cm^2 and inlet flow rate of 0.68 L/min. Hexahedral mapped mesh was adopted for the purpose of convergence speed and computing accuracy. Several meshes selected with grid numbers have been checked, as listed at Table 2. The calculated values T_{max}, the mean Nusset number Nu and the mean flow resistance coefficient fRe with different mesh are compared. The relative errors such as $E(T_{\mathrm{max}})$, $E(Nu)$ and $E(fRe)$ at different meshes are within 5%. Considering the calculation time cost and accuracy, the selected grid number is 2024845.

Table 2: Calculation and comparison of maximum temperature T_{max} of CPU chip, *Nu* number and *fRe* number of microchannel heat sink under different grid numbers

Grid number	1263138	2024845	319569
T_{max}	345.81	347.32	348.49
$E(T_{max})$	0.77%	0.34%	–
Nu	35.18	35.38	35.88
$E(Nu)$	1.95%	1.39%	–
fRe	11079	10970	10682
$E(fRe)$	3.72%	2.70%	–

3 Results and Discussion

In the present work, the microchannel heat sink modules are built with three fin heights H_f, i.e., 2 mm, 4 mm and 6 mm. The emitted heat fluxes q_m from the bottom of CPU are 10 W/cm^2, 20 W/cm^2, 30 W/cm^2, 40 W/cm^2 and 50 W/cm^2. The flow rates V_{in} of the cooling water are 0.21 L/min, 0.33 L/min, 0.45 L/min, 0.57 L/min and 0.68 L/min.

3.1 Heat Transfer Characteristics

In order to prevent the CPU operated at an overheated temperature, it is necessary to ensure that the maximum temperature T_{max} of CPU is lower than the limited temperature T_{lim} (i.e., 348.15 K). The corresponding heat flux emitted from the CPU is called the limited heat flux.

As depicted in Fig. 2, the maximum temperature T_{max} of CPU increases linearly with the heat flux q_m, while it is inversely proportional to the flow rate V_{in}. it is obvious that the max temperature T_{max} will exceed the limit temperature at large heat flux or small flow rate. For the fin height is $H_f = 2$ mm, the limited heat fluxes are about 32 W/cm^2 and 40 W/cm^2 when the flow rates are 0.21 L/min and 0.33 L/min. When the limited heat flux is 50 W/cm^2, the flow rate reaches at 0.68 L/min. Moreover, the increase in fin height is helpful to improve the limiting heat flux. When the flow rate is fixed at 0.33 L/min, the limited heat flux is 40 W/cm^2 at $H_f = 2$ mm, while the limited heat flux is about 50 W/cm^2 at $H_f = 4$ mm and 6 mm.

Figs. 3a and 3b display the surface and inner temperature profiles of the microchannel heat sink when the fin height, flow rate and heat flux are respectively 4 mm, 0.33 L/min and 30 W/cm^2. The temperature distribution of CPU chip is uneven. The part of the area with low temperature is near the inlet, while the high temperature zone locates at the opposite side. The temperature difference of the whole heat sink reaches 33 K.

Fig. 4 indicates the Nusselt number Nu is in positive proportion to the flow rate V_{in} and the heat flux q_m. It implies that the increase of flow rate and heat flux is beneficial to the improvement in heat transfer capacity of the microchannel heat sink. Moreover, both the magnitude and increment of the Nu number at $H_f = 2$ mm are larger than those at $H_f = 4$ mm and $H_f = 6$ mm. For example, when the heat flux is $q_m = 10$ W/cm^2 the Nu number is 32∼35 at $H_f = 2$ mm, while Nu number is 18∼22 at $H_f = 4$ mm and 15∼21 at $H_f = 6$ mm. Therefore, it is found that the microchannel heat sink with smaller fin height shows the better heat transfer capacity [22–27].

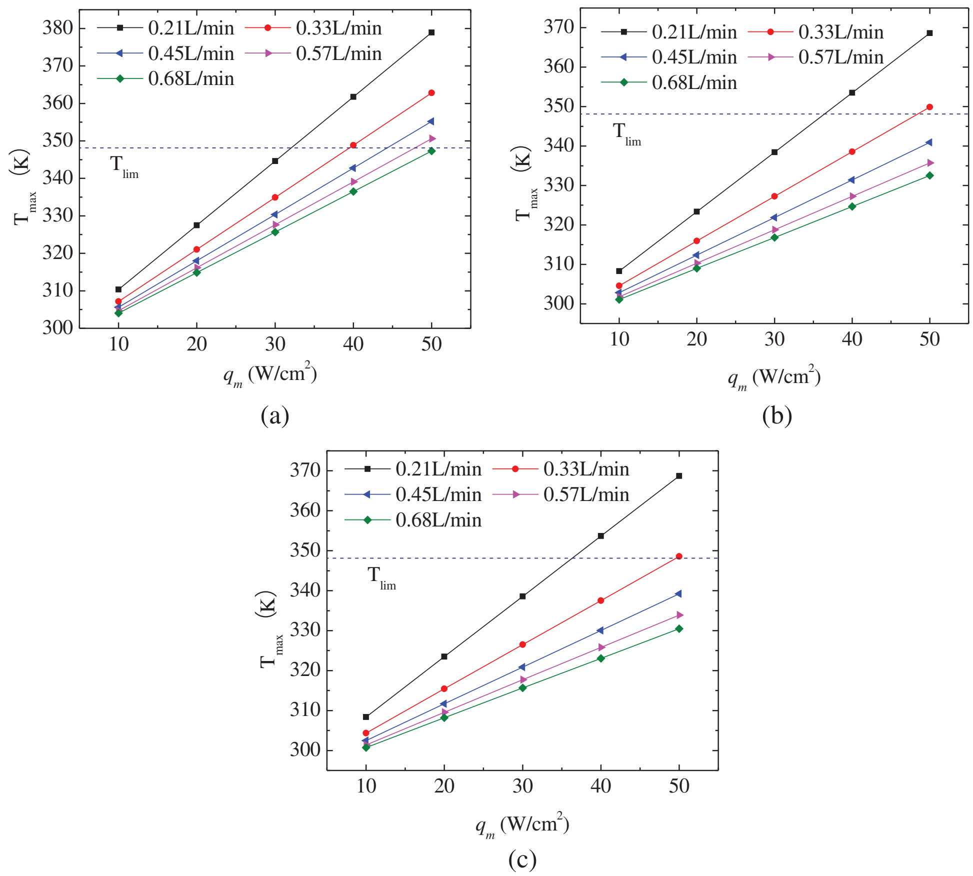

Figure 2: Variation of maximum temperature on the surface CPU chip with fin height of 2 mm (a), 4 mm (b) and 6 mm (c)

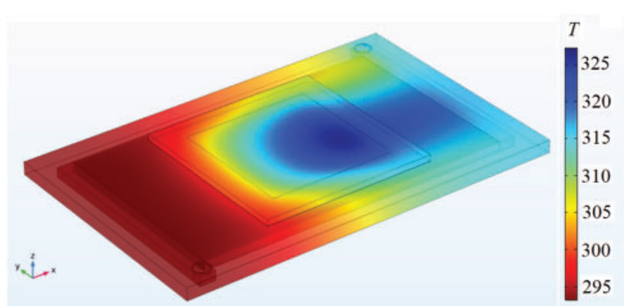

(a)

Figure 3: (Continued)

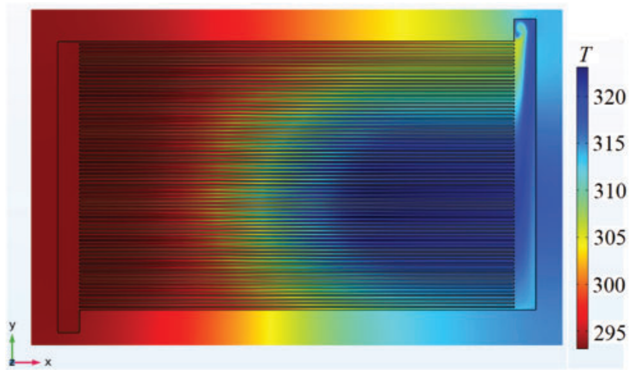

(b)

Figure 3: Temperature profiles of the whole microchannel heat sink (a) and the cross-section at $z = 2$ mm (b) when the fin height, flow rate and heat flux are respectively 4 mm, 0.33 L/min and 30 W/cm^2

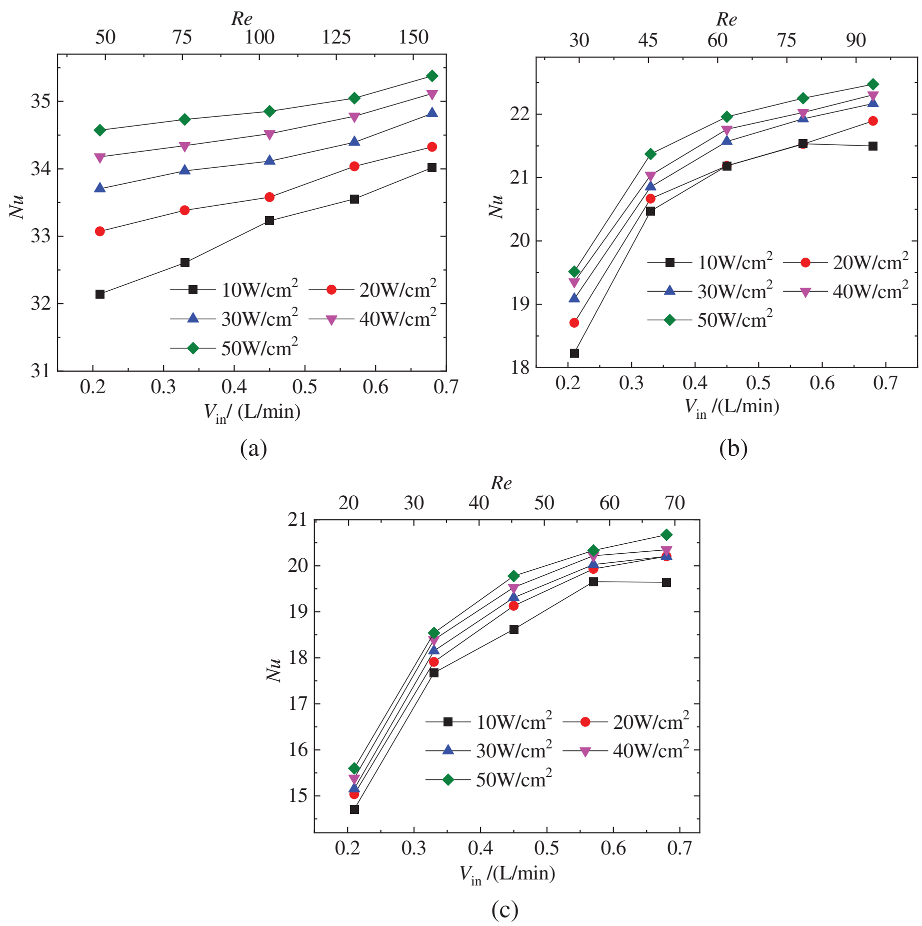

Figure 4: Variation of *Nu* number with the flow rate at fin heights of 2 mm (a), 4 mm (b) and 6 mm (c)

3.2 Flow Resistance Characteristics

The product of resistance coefficient and Reynolds number *fRe* is universal reference to reflect the corresponding flow losses for different types of heat sink [28,29]. As depicted in Fig. 5, the *fRe* value is almost linearly grows with the flow rate V_{in} at the considered fin heights and heat fluxes. When the fin height is 2 mm, the linear slops of the *fRe* to V_{in} are larger than those at $H_f = 4$ mm and at $H_f = 6$ mm. It is also found that the *fRe* values at $H_f = 2$ mm are about ten times larger than those at $H_f = 6$ mm. For instance, when V_{in} is 0.7 L/min and q_m is 10 W/cm^2, the *fRe* value is about 6.3×10^4 at $H_f = 2$ mm, while the *fRe* values is about 6.0×10^3 at $H_f = 6$ mm, respectively. Furthermore, the *fRe* value decreases with the heat flux. The increment of *fRe* with q_m is also reduced with the increase of fin height.

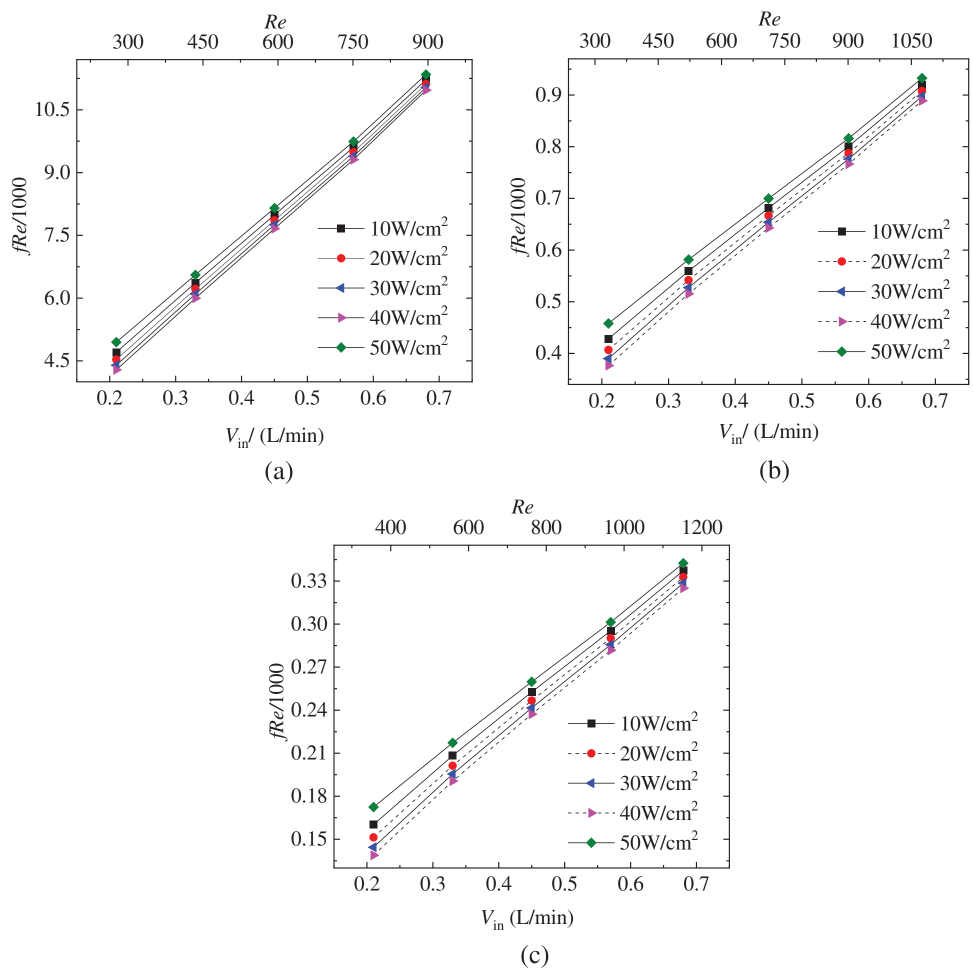

Figure 5: Variation of *fRe* with the flow rate V_{in} at fin height of $H_f = 2$ mm (a), 4 mm (b) and 6 mm (c)

3.3 Analysis on Convective Thermal Performance

JF factor [19–21,24] is the product of *j* factor and resistance coefficient *f*, which is utilized to evaluate the comprehensive efficiency of convective heat transfer and pressure drop in the microchannel heat sink. The *JF* factor is defined as:

$$JF = \frac{j/j_{\mathrm{R}}}{(f/f_{\mathrm{R}})^{1/3}}, \tag{8}$$

where, the subscript R means the reference case. Obviously, the larger value of the *JF* factor denotes a better the convective thermal performance of the microchannel heat sink. Furthermore, the analysis on convective thermal performance in the present work is conducted among the cases that the maximum temperature $T_{\max}$ of the CPU chip is less than the limited temperature.

Fig. 6 indicates the variation of *JF* factor with the flow rate and heat flux at different fin heights. When the fin height is $H_{\mathrm{f}} = 2$ mm, the reference case is $V_{\mathrm{in}} = 0.21$ L/min and $q_{\mathrm{m}} = 10$ W/cm^2, hence the corresponding *JF* factor is fixed at 1. As shown in Fig. 6a, the *JF* factors are less than 1 for all the considered flow rate larger than 0.21 L/min, except for the two cases of $q_{\mathrm{m}} = 20$ W/cm^2 and 30 W/cm^2 at $V_{\mathrm{in}} = 0.21$ L/min. The *JF* factor at different flow rate is monotonically increasing with the heat flux, however, it decreases with the flow rate. The values of *JF* factor at $V_{\mathrm{in}} = 0.68$ L/min are less than 0.4 when $H_{\mathrm{f}} = 2$ mm, which is resulted from the great flow resistance at large flow rates as shown in Fig. 5a. When the fin height increases, the number of operating case that $T_{\max}$ is less than limited temperature increases at $V_{\mathrm{in}} = 0.33$ L/min, as shown in Figs. 5b and 5c. Similarly, there are only two cases that the *JF* factor is larger than unit, i.e., $q_{\mathrm{m}} = 20$ W/cm^2 and 30 W/cm^2 at $V_{\mathrm{in}} = 0.21$ L/min. Moreover, *JF* factor is proportional to the heat flux at $H_{\mathrm{f}} = 4$ mm and $H_{\mathrm{f}} = 6$ mm, while it is inversely proportional to the flow rate.

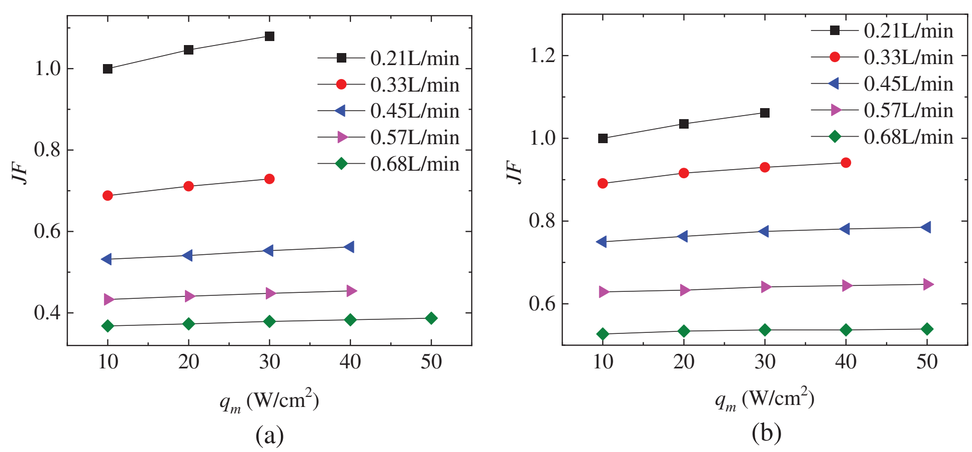

Figure 6: (Continued)

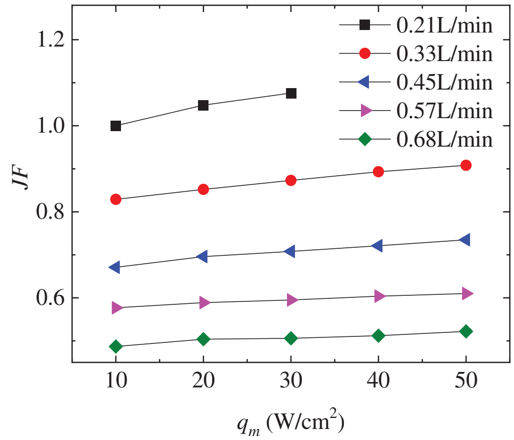

(c)

Figure 6: Variation of JF factor with the flow rate and heat flux at fin height of $H_f = 2$ mm (a), 4 mm (b) and 6 mm (c)

In order to determine the optimal operating case for the present, further evaluation has been conducted by selecting the best convective thermal performance at each heat flux within three fin heights. For instance, when the heat flux is 10 W/cm^2, the best case is $V_{in} = 0.21$ L/min at three fin heights. When the heat flux is 50 W/cm^2, the best cases are $V_{in} = 0.68$ L/min, 0.45 L/min and 0.33 L/min at $H_f = 2$ mm, 4 mm and 6 mm, respectively. As indicated in Fig. 7, the case at $H_f = 4$ mm is the reference case, hence the corresponding JF factor equals to 1. Results show that when the heat flux is less than or equal 30 W/cm^2, the optimal operating case is at $V_{in} = 0.21$ L/min and $H_f = 2$ mm. When heat flux is 40 W/cm^2 or 50 W/cm^2, the optimal operating case is at $V_{in} = 0.33$ L/min and $H_f = 6$ mm. It implies that the microchannel with short fins shows optimal convective thermal performance when the thermal power of CPU chip is small. The fins should heighten when the CPU is operating at higher thermal power.

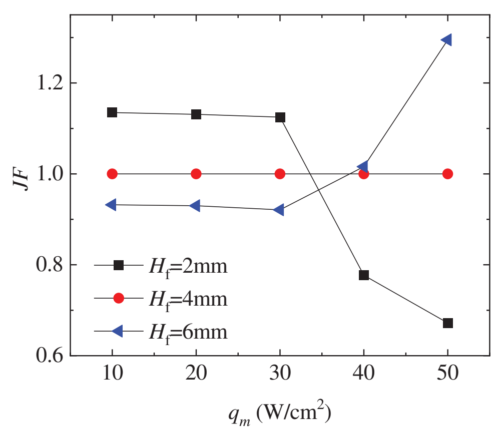

Figure 7: Comparison of JF factor among the selected case with best convective thermal performance at each heat flux within three fin heights

4 Summary and Conclusions

To reveal the effects of heat flux, fin height and flow rate on convective thermal performance of microchannel heat sinks, the fluid flow and heat transfer were numerically investigated and the *JF* factor were employed to evaluate the heat transfer characteristic. Main conclusions are given as follows:

1. The maximum temperature of CPU chip increases with the heat flux. The increase in fin height and flow rate of cooling water is helpful to improve the limiting heat flux of CPU.
2. Large flow rate and heat flux and short fin height are benefit to improve the Nusselt number in the microchannel heat sink, but it results in large resistance coefficient *fRe* simultaneously.
3. The *JF* factor increases monotonically with the heat flux, but decreases with the flow rate. When the heat flux is less than or equal 30 W/cm^2, the optimal operating case is at $V_{in} = 0.21$ L/min and $H_f = 2$ mm. When heat flux is 40 W/cm^2 or 50 W/cm^2, the optimal operating case is at $V_{in} = 0.33$ L/min and $H_f = 6$ mm.

In general, the design of microchannel heat sink and the operating condition are very important to flow and heat transfer. The employment of *JF* factor shows its pertinence and convenience to evaluate the comprehensive convective thermal performance of microchannel heat sink.

Funding Statement: The work is supported by Doctoral Start-up Foundation of Dongguan University of Technology (GC300502-38), Guangdong Provincial Key Laboratory of Distributed Energy Systems (2020B1212060075), Natural Science Foundation of Guangdong Province (2019A1515110498, 2019A1515111167, 2021A1515110616) and Dongguan Institute of Technology quality Engineering (201802096).

Conflicts of Interest: The authors declare that they have no conflicts of interest to report regarding the present study.

References

1. Moore, G. E. (1998). Cramming more components onto integrated circuits. *Electronics, 86(1),* 82–85. DOI 10.1109/jproc.1998.658762.
2. Nakayama, W. (1986). Thermal management of electronic equipment: A review of technology and research topics. *Applied Mechanics Reviews, 39(12),* 1847–1868. DOI 10.1115/1.3149515.
3. Whelan, B. P., Kempers, R., Robinson, A. (2012). A liquid-based system for CPU cooling implementing a jet array impingement waterblock and a tube array remote heat exchanger. *Applied Thermal Engineering, 39,* 86–94. DOI 10.1016/j.applthermaleng.2012.01.013.
4. Shahsavar, A., Shahmohammadi, M., Askari, I. B. (2003). CFD simulation of the impact of tip clearance on the hydrothermal performance and entropy generation of a water-cooled pin-fin heat sink. *International Communications in Heat and Mass Transfer, 126,* 105400.
5. Shen, H., Xie, G. N., Wang, X. X. (2020). Thermal performance and entropy generation of novel Xstructured double layered microchannel heat sinks. *Journal of the Taiwan Institute of Chemical Engineers, 111,* 90–104.
6. Arani, A. A. A., Akbari, O. A., Safaei, M. R., Marzban, A., Alrashed, A. et al. (2017). Heat transfer improvement of water/single-wall carbon nanotubes (SWCNT) nanofluid in a novel design of a truncated double-layered microchannel heat sink. *International Journal of Heat and Mass Transfer, 113(9),* 780–795. DOI 10.1016/j.ijheatmasstransfer.2017.05.089.

7. Bare, P. A., Abubakar, S. B., Sidik, N. A. (2015). Numerical prediction of laminar nanofluid flow in rectangular microchannel heat sink. *Journal of Advanced Research in Fluid Mechanics and Thermal Sciences, 7,* 29–38.
8. Barrau, J., Chemisana, D., Rosell, J., Tadrist, L., Ibañez, M. (2010). An experimental study of a new hybrid jet impingement/micro-channel cooling scheme. *Applied Thermal Engineering, 30(14),* 2058–2066. DOI 10.1016/j.applthermaleng.2010.05.013.
9. Alihosseini, Y., Targhi, M. Z., Heyhat, M. M., Ghorbani, N. (2020). Effect of a micro heat sink geometric design on thermo-hydraulic performance: A review. *Applied Thermal Engineering, 170(4),* 114974. DOI 10.1016/j.applthermaleng.2020.114974.
10. Toh, K. C., Chen, X., Chai, J. (2002). Numerical computation of fluid flow and heat transfer in microchannels. *International Journal of Heat and Mass Transfer, 45(26),* 5133–5141. DOI 10.1016/S0017-9310(02)00223-5.
11. Tuckerman, D. B. (1981). High-performance heat sinking for VLSI. *IEEE Electron Device Letters, 2(5),* 126–129. DOI 10.1109/EDL.1981.25367.
12. Ying, H. E., Shao, B. D., Cheng, H. M. (2014). Numerical simulation and size optimization of rectangular micro-channel heat sinks. *Applied Mathematics Mechanics, 35(3),* 568–573. DOI 10.3879/j.issn.1000-0887.2014.03.006.
13. Xie, G. N., Li, S. A., Sunden, B., Zhang, W. H. (2014). A numerical study of the thermal performance of microchannel heat sinks with multiple length bifurcation in laminar liquid flow. *Numerical Heat Transfer, Part A: Applications, 65(2),* 107–126. DOI 10.1080/10407782.2013.826084.
14. Gong, L., Zhao, J., Huang, S. (2015). Numerical study on layout of micro-channel heat sink for thermal management of electronic devices. *Applied Thermal Engineering, 88(3),* 480–490. DOI 10.1016/j.applthermaleng.2014.09.048.
15. Al-Neama, A. F., Kapur, N., Summers, J., Thompson, H. M. (2017). An experimental and numerical investigation of the use of liquid flow in serpentine microchannels for microelectronics cooling. *Applied Thermal Engineering, 116(4),* 709–723. DOI 10.1016/j.applthermaleng.2017.02.001.
16. Khoshvaght-Aliabadi, M., Hassani, S. M., Mazloumi, S. H. (2017). Comparison of hydrothermal performance between plate fins and plate-pin fins subject to nanofluid-cooled corrugated miniature heat sinks. *Microelectronics Reliability, 70(2),* 84–96. DOI 10.1016/j.microrel.2017.01.005.
17. Liu, H. L., Guo, H. Y., Xie, Z. L., Sang, L. (2021). Numerical investigations for optimizing a novel microchannel sink with perforated baffles and perforated walls. *International Communications in Heat and Mass Transfer, 126,* 105342. DOI 10.1016/j.icheatmasstransfer.2021.105342.
18. Mazloumi, H. S., Hassani, M. S., Khoshvaght-Aliabadi, M. (2017). Comparison of hydrothermal performance between plate fins and plate-pin fins subject to nanofluid-cooled corrugated miniature heat sinks. *Microelectronics Reliability, 70(2),* 84–96. DOI 10.1016/j.microrel.2017.01.005.
19. Li, K., Wen, J., Yang, H., Wang, S., Li, Y. (2019). Sensitivity and stress analysis of serrated fin structure in plate-fin heat exchanger on cryogenic condition. *International Journal of Thermal Sciences, 145(3),* 106013. DOI 10.1016/j.ijthermalsci.2019.106013.
20. Al-Zahrani, S., Islam, M. S., Saha, S. C. (2021). Comparison of flow resistance and port maldistribution between novel and conventional plate heat exchangers. *International Communications in Heat and Mass Transfer, 123(9),* 105200. DOI 10.1016/j.icheatmasstransfer.2021.105200.
21. Mohebbi, S., Veysi, F. (2021). Numerical investigation of small plate heat exchangers performance having different surface profiles. *Applied Thermal Engineering, 188(8),* 116616. DOI 10.1016/j.applthermaleng.2021.116616.
22. Zhao, Z., Li, L., Pu, Z., Ju, Z. (2015). Optimal design of water-cooled micro-channel radiator for chips. *Refrigeration Air-Conditioning, 15(5),* 32–37.

23. Toh, K. C., Chen, X. Y., Chai, J. C. (2002). Numerical computation of fluid flow and heat transfer in microchannels. *International Journal of Heat and Mass Transfer, 45(26),* 5133–5141. DOI 10.1016/S0017-9310(02)00223-5.
24. Yun, J. Y., Lee, K. S., Wang, Y. H. (2000). Influence of design parameters on the heat transfer and flow friction characteristics of the heat exchanger with slit fins. *International Journal of Heat and Mass Transfer, 43(14),* 2529–2539. DOI 10.1016/S0017-9310(99)00342-7.
25. Gong, L., Zhao, J., Huang, S. (2015). Numerical study on layout of micro-channel heat sink for thermal management of electronic devices. *Applied Thermal Engineering, 88(3),* 480–490. DOI 10.1016/j.applthermaleng.2014.09.048.
26. Kwon, H., Joo, Y., Kim, S. J. (2018). Analytic approach to thermal optimization of horizontally oriented radial plate-fin heat sinks in natural convection. *Energy Conversion and Management, 156,* 555–567. DOI 10.1016/j.enconman.2017.11.076.
27. Buyruk, E., Karabulut, K., Karabulut, Ö. O. (2013). Three-dimensional numerical investigation of heat transfer for plate fin heat exchangers. *Heat and Mass Transfer, 49(6),* 817–826. DOI 10.1007/s00231-013-1129-8.
28. Ghani, I. A., Sidik, N., Kamaruzaman, N. (2017). Hydrothermal performance of microchannel heat sink: The effect of channel design. *International Journal of Heat and Mass Transfer, 107,* 21–44. DOI 10.1016/j.ijheatmasstransfer.2016.11.031.
29. Zhou, J., Cao, X., Zhang, N., Yuan, Y., Zhao, X. et al. (2020). Micro-channel heat sink: A review. *Journal of Thermal Science, 29(6),* 1431–1462. DOI 10.1007/s11630-020-1334-y.